Proceedings of the International Association for Shell and Spatial Structures (IASS) Symposium 2009, Valencia
Evolution and Trends in Design, Analysis and Construction of Shell and Spatial Structures
28 September – 2 October 2009, Universidad Politecnica de Valencia, Spain
Alberto DOMINGO and Carlos LAZARO (eds.)

Deployment Simulation of Inflatable Structures Based on Improved Spring-mass System

Yan XU*, Fuling GUAN

College of Architecture and Civil Engineering
Zijingang Campus, Zhejiang University
Hangzhou, P.R.CHINA, 310058
Email Address: *xyzs@zju.edu.cn

Abstract

Inflatable membrane antenna structures are applied in spaceflight missions broadly. Fold and deployment simulation of inflatable antenna is the key technology of structure analysis. The simulation method of membrane deployable structure is mentioned based on improved spring-mass system. During structure development, self-contact or collision of membrane film may occur easily. The distinguish rule of self-contact elements is advanced and penalty function method is used to solve this difficult problem. Finite different method is used to solve the motion of system. Membrane inflatable tube is one of most important members for spatial inflatable structure. These time history of inflatable pressure and other gas parameter of each tube part are analyzed. The tube between two hinges is equal to cantilever beams and the moment tending to straighten the tube is obtained. This deployable moment is equal to drive forces which subjected to the spring-mass system. Numerical examples are presented to show that analyze method can simulate the 3D deployment motion of inflatable tube. Compared to the experiment result from the reference, the validity of the method is shown and the analysis precision is high. Then initial state and fold state of main members of inflatable antenna are described, which include inflatable tube, inflatable torus and reflector etc. Deployable drive forces and deployable process order of each part are analyzed. The antenna model like IAE antenna is analyzed and simulated by the fore mentioned system. Each state during deployment process and velocity and acceleration of each node are obtained. The example is used to validate the simulation method and the fold scheme of inflatable antenna.

Keywords: inflatable antenna, deployment simulation, spring-mass system, self-contact, fold pattern.

1. Introduction

Large size spaceflight structures are difficult to achieve because the limitation of weight and launch volume. Compared to the rigid deployable antenna structures[1], the inflatable antenna structures have many advantages including design flexibility, light weight, and compact launch volume and are fit for large size spaceflight structures.

From 1990s, inflatable technologies are used to antenna structure by NASA's Jet Propulsion Laboratory etc. Many ideas, concepts and models are arisen such as waveguide array antenna and hybrid inflatable dish antenna [2-4].

The deployable simulation and research of inflatable structure is almost about infltable tube. There are two main simulation method multi-rigid-body dynamic[5-8] and dynamic nonlinear finit element[9-12]. The second method is used popularly. A. L. Clem.etc[7-8] considered the tube between two fold point as inflatable cantilever beams and analyze by multi-rigid-body dynamic. Haug PAM-CRASH.etc[9] used software PAM-CRASH to simulation the deployment of inflatable structure. Salama[10] used software LSDYNA to analyze the deployment of tube and considered the reciprocity between gas flow and flexible tube shell. J. T. Wang.etc[11-12] analyzed the deployment of tube by FEM software. Yasuyuki Miyazaki.etc[13] analyzed the deployment of tube by contact mechanics and hydrodynamics and experiment for a tube with one fold point.

The simulation method of membrane deployable structure in this thesis is mentioned based on improved spring-mass system. The whole antenna structure include tube, torus and reflector is simulated by the method. The self-contact problem, the inflatable pressure and deployable moment analysis are most important parts in this work.

2. inflatable simulation method

2.1 spring-mass system description

A spring-mass system is established to describe membrane material. The three vertexes of the membrane triangle element are masses and three borders are springs. The lengths of springs in initial estate are of the original lengths. During the deployment process, the spring lengths are not equal to their original lengths, so that internal forces exist in these springs. The three masses move under the combined action of the spring forces and external forces to reach the final equilibrium state. Spring-mass system in an element is shown in Fig. 1. The mass of mass point i is determined by the area of membrane elements, as shown in Fig2:

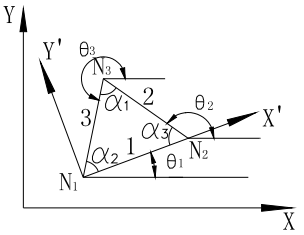

Fig 1: Spring-mass system

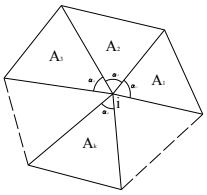

Fig 2:triangle elements around mass i

$$m_i = \frac{\alpha_i \cdot \rho}{2\pi} \sum_{k=1}^{s} A_k \tag{1}$$

Where ρ is the area density of the material; A_k is the area of element k around mass point i; s is the number of elements around mass i; α_i is the internal angle each vertex of the element.

The tension vector of springs in the element can be obtained from

$$\begin{Bmatrix} T_1 \\ T_2 \\ T_3 \end{Bmatrix} = \mathbf{B}^T \mathbf{D} \mathbf{B} \begin{Bmatrix} \delta_1 \\ \delta_2 \\ \delta_3 \end{Bmatrix} V \tag{2}$$

Where $\mathbf{T}, \boldsymbol{\delta}$ are tension force vector and extension vector of three springs respectively, V is the volume of triangle element.

$$\mathbf{D} = \begin{bmatrix} d_{11} & d_{12} & 0 \\ d_{21} & d_{22} & 0 \\ 0 & 0 & d_{33} \end{bmatrix} \tag{3}$$

$d_{11} = d_{22} = E/(1-\nu^2), d_{12} = d_{21} = \nu E/(1-\nu^2), d_{33} = E/2(1+\nu)$

Where E isYoung's modulus, v is Poisson's ratio.

$$\mathbf{B} = \frac{1}{|\mathbf{A}|} \begin{bmatrix} (b_2c_3 - b_3c_2)l_1^{-1} & (b_3c_1 - b_1c_3)l_2^{-1} & (b_1c_2 - b_2c_1)l_3^{-1} \\ (a_3c_2 - a_2c_3)l_1^{-1} & (a_1c_3 - a_3c_1)l_2^{-1} & (a_2c_1 - a_1c_2)l_3^{-1} \\ (a_2b_3 - a_3b_2)l_1^{-1} & (a_3b_1 - a_1b_3)l_2^{-1} & (a_1b_2 - a_2b_1)l_3^{-1} \end{bmatrix} \quad a_i = \cos^2\theta_i, b_i = \sin^2\theta_i, c_i = \sin\theta_i \cos\theta_i$$

$$\mathbf{A} = \begin{bmatrix} a_1 & b_1 & c_1 \\ a_2 & b_2 & c_2 \\ a_3 & b_3 & c_3 \end{bmatrix}$$

Where l_i are spring initial lengths and θ_i are angles that the sides of the element make with the X-axis.

2.2 self-contact problem

During structure deployment, contact and collide of membrane films may occur, which is commonly referred to as the self-contact problem. To prevent self-contact, a penalty force is added to these masses. Adapting Provot's method, when the mass A moves to a position that is too close to the element plane IJK, the penalty function is applied to the position of the mass to prevent collision, shown in fig3. If the project node A' is in the triangle element field, there is a contact relationship between mass A and element IJK. The penalty force for the mass A is defined as follows:

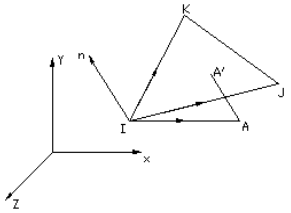

Fig 3: Self-contact element

$$\mathbf{F}_P = \sum_{j=1}^{m} C_P \left| h_j - h_j^* \right| \mathbf{n} \tag{4}$$

$$C_P = \begin{cases} 1 & (h_j \le h_j^*) \\ 0 & (h_j > h_j^*) \end{cases} \tag{5}$$

Where $\mathbf{F}_P$ is the penalty force vector for the mass A, C_p is the penalty coefficient, h_j is the current distance from the mass A to the element plane ijk, h_j^* is a fixed value, and n is the unit normal vector.

If the project node A' is not in the triangle element field, there will not be any contact between mass A and element IJK.

2.3 equation of deployment dynamic

The equation of motion for masses subjected to internal and external forces is given as follows.

$$\mathbf{M}\ddot{\mathbf{X}} + \mathbf{C}\dot{\mathbf{X}} + \mathbf{K}\mathbf{X} = \mathbf{F}_{\mathrm{I}} + \mathbf{F}_{\mathrm{E}} \tag{6}$$

Where $\mathbf{M}, \mathbf{C}, \mathbf{K}$ are mass, damping and stiffness matrices, respectively, $\mathbf{F}_I$ is the inertial force arising from the dynamic coupling between the local and global degrees of freedom, and $\mathbf{F}_E$ is the generalized external force associated with the degrees of freedom of the model. $\mathbf{X}$ is the position vector of all masses.

For each mass, there are

$$m\frac{\partial^2 X}{\partial t^2} + c\frac{\partial X}{\partial t} = F_{ex} + F_{in} \tag{7}$$

From Finite different method, these two left terms of the upper equation can be simpled as

$$m\frac{\partial^2 X}{\partial t^2} = m\frac{1}{\Delta t^2}(X_{t+\Delta t} - 2X_t + X_{t-\Delta t}), c\frac{\partial X}{\partial t} = c\frac{1}{2\Delta t}(X_{t+\Delta t} - X_{t-\Delta t}) \tag{8}$$

Substituting Equ. (8) into (7) yields

$$m\frac{1}{\Delta t^2}(X_{t+\Delta t} - 2X_t + X_{t-\Delta t}) + c\frac{1}{2\Delta t}(X_{t+\Delta t} - X_{t-\Delta t}) = F_{ex} + F_{in} \tag{9}$$

$$(m\frac{1}{\Delta t^2}+c\frac{1}{2\Delta t})X_{t+\Delta t}=F_{ex}+F_{in}+m\frac{2}{\Delta t^2}X_t-(m\frac{1}{\Delta t^2}-c\frac{1}{2\Delta t})X_{t-\Delta t} \tag{10}$$

Given

$$M=m\frac{1}{\Delta t^2},C=c\frac{1}{2\Delta t},F=F_{ex}+F_{in}$$

Then for the whole spring-mass system, there is:

$$(\mathbf{M}+\mathbf{C})\mathbf{X}_{t+\Delta t}=\mathbf{F}_{ex}+\mathbf{F}_{in}+2\mathbf{M}\mathbf{X}_t-(\mathbf{M}-\mathbf{C})\mathbf{X}_{t-\Delta t} \tag{11}$$

The initial configuration of the system is static state. Then displacement, velocity and acceleration at time 0 are zero.

$$\mathbf{X}_t\big|_{t=0}=0,\mathbf{X}_{t-\Delta t}\big|_{t=0}=0,\frac{\partial \mathbf{X}_t}{\partial t}\bigg|_{t=0}=0,\frac{\partial^2 \mathbf{X}_t}{\partial t^2}\bigg|_{t=0}=0 \tag{12}$$

The initial state of the deployment process is the fold configuration Ω_0 of the membrane structure. Membrane film deploys to the state Ω_i by Eq.(7). Eq.(1).(2) are used to compute the mass of each mass and internal force of each spring. To solve the self-contact problem, the penalty force from Eq.(4) is added to the system.

3.The analysis of infltable pressure

It is further assumed that the temperature and pressure of the gas are uniform within the control volume of an individual boom compartment. As a result, is valid for each compartment.

$$P_iV_i=m_iRT_i \tag{13}$$

In equation one, and denote pressure, volume, mass, and temperature of the i compartment and R is the gas constant.

The rate of mass changing of the icompartment at time t is determined by

$$\frac{dm_i}{dt}=\dot{m}_{in}-\dot{m}_{out}=\dot{m}_{hi}-\dot{m}_{ij} \tag{14}$$

where subscript i denotes the current compartment, h denotes the previous compartment, and j denotes the next compartment. is the mass rate of gas flowing into the i compartment from hcompartment and is the mass rate of gas flowing out from the i compartment to j compartment.

The mass flow rate from one compartment to the next compartment is approximated by one-dimensional, quasi-steady, isentropic flow and formulated as,

$$\frac{dm_{ij}}{dt}=A_{ij}\frac{P_i}{R\sqrt{T_i}}\left(\frac{P_e}{P_i}\right)^{\frac{1}{k}}\sqrt{2g\left(\frac{kR}{k-1}\right)\left(1-\left(\frac{P_e}{P_i}\right)^{\frac{k-1}{k}}\right)} \tag{15}$$

where $k = c_p / c_v$ is the specific heat ratio of the gas, A_{ij} is the connecting area between two compartments and

The critical pressure at which sonic flow occurs can be calculated by,

$$\frac{P_c}{P_i} = \left(\frac{2}{k+1} \right)^{\frac{k}{k-1}} \tag{16}$$

The pressure P_e in Equ is given by,

$$P_e = \begin{cases} P_j & P_j > P_c \\ P_c & P_j < P_c \end{cases} \tag{17}$$

The connecting area A_{ij} between compartment i and compartment j can be defined by,

$$A_{ij} = \begin{cases} 0 & V_i < r_i V_i^* \\ \dfrac{\left(\dfrac{V_i}{V_i^*} - r_i \right) A}{1 - r_i} & V_i \geq r_i V_i^* \end{cases} \tag{18}$$

where V_i^* is the fully inflated volume of the i compartment.

This equation represents the fact that the compartment j stays deflated until of the previous compartment, compartment i, has been filled. depend on the deployment control system (e.g. peel strength of the Velcro strips) and can be determined by experiment.

The state (pressure, volume, temperature, and mass) of each compartment can be determined by the first law of thermodynamics. For an adiabatic process,

$$\frac{d}{dt}\left(m_j c_v T_j \right) = c_p T_i \dot{m}_{in} - c_p T_j \dot{m}_{out} - P_j \frac{dV_j}{dt} \tag{19}$$

where c_v and c_p are the specific heat of the gas with constant volume and pressure, and j=i+1. On the other hand,

$$\frac{d}{dt}\left(m_j c_v T_j \right) = m_j c_v \frac{dT_j}{dt} + c_v T_j \frac{dm_j}{dt} \tag{20}$$

Combining equations (18) and (19) with (13) yields,

$$\frac{\dot{T}_j}{T_j} = \frac{1}{m_j}\left(\dot{m}_{out} - \dot{m}_{in} \right) + \frac{k}{m_j}\left(\frac{T_i}{T_j} \dot{m}_{in} - \dot{m}_{out} \right) - \frac{(k-1)}{V_j} \dot{V}_j \tag{21}$$

The pressure of compartment j is defined by

$$P_j = P_a + (P_i - P_a)\frac{V_j}{V_j^*} \tag{22}$$

where P_a is the environmental pressure and V_j^* is the fully deployed volume of the j compartment. Equation (22) means that, the pressure of j^{th} compartment equals to the environmental pressure before it starts to deploy and equals to the pressure of the previous compartment after it is fully deployed. The derivative of equation (22) is,

$$\dot{P}_j = \dot{P}_i\frac{V_j}{V_j^*} + (P_i - P_a)\frac{\dot{V}_j}{V_j^*} \tag{23}$$

For every compartment, a group of differential governing equations can be obtained from equations (14), (15), (18), (22), (23) and expressed as,

$$\begin{bmatrix} 0 & 0 & 0 & 0 & m_j V_j & V_j T_j & 0 & (k-1)m_j T_j \\ 0 & 0 & 0 & 0 & 0 & 1 & 0 & 0 \\ 0 & 0 & 0 & 0 & -m_j R & -RT_j & V_j & P_j \\ 0 & 0 & V_j & 0 & 0 & 0 & -V_j^* & (P_i - P_a) \end{bmatrix} \begin{Bmatrix} \dot{T}_i \\ \dot{m}_i \\ \dot{P}_i \\ \dot{V}_i \\ \dot{T}_j \\ \dot{m}_j \\ \dot{P}_j \\ \dot{V}_j \end{Bmatrix} = \begin{Bmatrix} kT_i V_j \dot{m}_{in} - kT_j V_j \dot{m}_{out} \\ \dot{m}_{in} - \dot{m}_{out} \\ 0 \\ 0 \end{Bmatrix} \tag{24}$$

Where $\dot{m}_{in}, \dot{m}_{out}$ can be calculated by equation (14). The state of each compartment is then calculated by integrating this group of differential equations with respect to time. Runge-Kutta method has been used by this study to numerically integrate this group of differential equations.

4.The analysis of deployable moment

It is clear that the strut curvature at hinge A and hinge is very large and are opposite sign. Then there have to be a zero section in tube between hings A and B. It is assumed that there is only one curvature section between two hings and it is titled as hing C, shown as Fig 3. during deployment process, the maximum curvture is at the hinge point B and the tip C has zero curvature. So the tube B-C can be considered as inflatable cantilever beams.

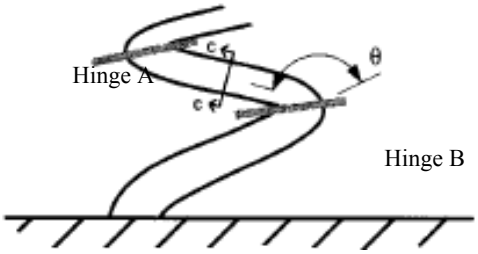

Fig4: the deployable moment of fold hinge

Based on the upper assumption, the relationship between the fold angle and deploy moment is proved. Similar to the bending of an cantilever strut subjected to an increasing tip load, the curvature is at a maximum value at the base and zero at the tip. It is assumed that the moment causing the tube to curve in the case of the cantilever is equal and opposite the moment tending to straighten out the tube during deployment.

Based on Bernoulli-Euler method, there is the differential equation of solid elastic beams:

$$\frac{d^2y}{dx^2}=\frac{M+2\nu pr^3\sin\varphi}{Etr^3[(\pi-\varphi)+\sin\varphi\cos\varphi]} \tag{25}$$

Where y is deflection of beam, x is the local coordinate of beam, M is the deploy moment in fold point, E is elastic modulus of membrane material, ν is Poisson's ratio, t is the thickness, p is the pressure in the tube, φ is the half angle of wrinkle region around the circumference of the inflated tube.

The relationship equation between the moment M and the angle φ is:

$$\frac{M}{pr^3}=\frac{\pi/2[(\pi-\varphi)+\sin\varphi\cos\varphi]-\nu[(\pi-\varphi)^2-(\pi-\varphi)\sin\varphi\cos\varphi-2\sin^2\varphi]}{\sin\varphi+(\pi-\varphi)\cos\varphi} \tag{26}$$

The coupling equations are nondimensionalized:

$$Y=\frac{Et}{p}y(x) \tag{27}$$

where

$$T=\frac{M}{pr^3}\ ,\ F(T,\varphi)=\frac{T+(2\gamma/\pi)\sin\varphi}{1/\pi[(\pi-\varphi)+\sin\varphi\cos\varphi]} \tag{28}$$

Where Y is a dimensionless displacement, T is a dimensionless moment and F is a dimensionless curvature fuction.

Equ.(27) becomes:

$$Y'' = F(T, \varphi) \tag{29}$$

Subjected to these constraint conditions:

$T < (1-2\nu)/2$ for $\varphi = 0$

$(1-2\nu)/2 < T < 1$ for

$$T = \frac{1/2[(\pi-\varphi)+\sin\varphi\cos\varphi] - \nu/\pi[(\pi-\varphi)^2 - (\pi-\varphi)\sin\varphi\cos\varphi - 2\sin^2\varphi]}{\sin\varphi + (\pi-\varphi)\cos\varphi}$$

The rrelationship fuction between the slop $Y^{*'}$ of the nondimensionalized cantilever and the dimensionless moment T is

$$T = (1 - e^{-3.12Y^{*'}}) \tag{30}$$

Substituting Equ. (28) and (29) into (30) yields

$$\frac{M}{\pi p r^3} = (1 - \exp(\frac{-3.12Et}{p} Y^{*'})) \tag{31}$$

The relationship between the slop $Y^{*'}$ and the angle from one link and the next(titled as fold angle) is

$$\tan\frac{\theta}{2} = Y^{*'} \tag{32}$$

Substituting Equ. (32) into (31) yields

$$M = \pi p r^3 [1 - \exp(\frac{-3.12Et}{p} \tan\frac{\theta}{2})] \tag{33}$$

This is denoted that the deploy moment M is a function of the fold angle θ and the inflatable pressure p .

5. Numerical model of fold configuration

5.1 inflatable tube

There are two fole pattern of inflatable tube commonly: the first is curve fold and the axial is discribed by the isometric line. The curve equation is:

$$\rho = be^{a\theta} \tag{34}$$

Where different coefficient a and b donates different fold configuration. The coefficient a image the degree of fold and The coefficient b is the radius of curve mandril.

For inflatable tube, the section of fold configuration is shown in Fig. The fold section is included two pieces of arc. R_1 is the section redius of unfold configuration and R_2 is the section redius of fold configuration. The strain of membrane material is ignored during fold

process, then the circumference length of tube is invariability. The centre angle of arc θ in fold configuration is:

$$\theta = \pi R_1 / R_2 \tag{35}$$

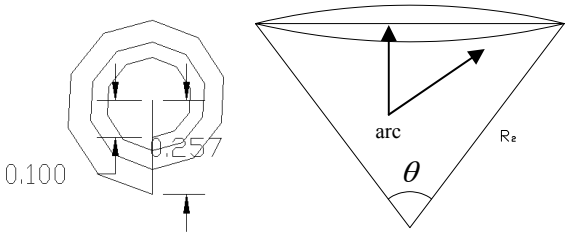

Fig 5: the axes and section of fold configuration for inflatable tube

So the coordination of each node in the arc can be calculated. The fold configuration of tube is numerical modeled, shown in Fig6. The second fold pattern is Z-fold, the numerical model of fold configuration is shown in Fig7.

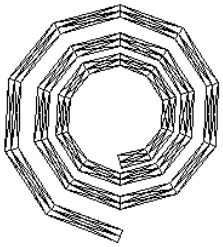

Fig 6: model of curve fold pattern

Fig 7: model of Z-fold pattern

Based on these upper thoeries, the depolyment simulation code for inflatable tube structure is compiled by Fortran. The simulation result is outputted to dxf. file and each depoly states is saved into different layer.

There are four kinds of states in the deployable simulation of inflatable antenna: non-stress state (before fold), fold state, full-deployable state and deployable state. The work of deployable simulation is each deployable state during deployable process and full-deployable state are obtained when non-stress state and fold state are known and the structure is subject to constraint condition and external force.

In following the non-stress state and fold state are numerical modeled for common components in inflatable antenna: tube, torus and inflatable reflector.

5.2Inflatable torus

The non-stress state of inflatable torus is cirque shell surface. Because the Gauss curvature of inflatable torus isn't zero, so it is un-fold surface and the initial stress is occur during fold process. As inflatable tube, the section shape of torus in non-stress state is circle and the section in fold state includes two pieces of arc.

The axes of torus is also circle and a new fold pattern is approved in this thesis. Circle curve is dispersed to polygon and Z-fold pattern is used to fold axes.

R is the radius of torus's axes. n is the fold number of axes. θ is fold angle. The length of each axes part is:

$$L = \frac{2\pi R}{n} \tag{36}$$

The projection shape in oxy plane is polygon after fold. The length of each border is:

$$L_{xy} = \frac{2\pi R}{n}\cos\theta \tag{37}$$

The radius of circumcircle is

$$r = L_{xy}\frac{R}{L} \tag{38}$$

The projection height in oxz plane is

$$L_{xz} = \frac{2\pi R}{n}\sin\theta \tag{39}$$

So the coordination of each fold point is:

$$x = r\cos\varphi, y = r\sin\varphi, z = \pm\frac{Lxz}{2} \tag{40}$$

Where φ is corresponding centre angle. The sign of z coordination is alternation selected.

5.3 inflatable reflector

The reflector is an air bag which include reflector and canopy. The shape of reflector is paraboloid surface when subject to inflatable pressure. It is difficult to fold paraboloid surface. The fold pattern for plane membrane in reference is used to fold reflector surface. Because paraboloid surface is revolve surface, so the surface is folded along longitude and latitude direction. The fold pattern along latitude direction is similar to the axes direction of inflatable torus.

The fold pattern of canpoy is similar to the reflector surface. The canpoy is near by the reflector and Z coordination of each point in canpoy is smaller 1mm to the corresponding point in reflector.

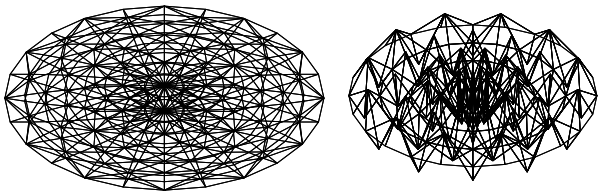

Fig 8: The non-stress and fold state of reflector

6. Deployable simulation of antenna structure

6.1 Z- fold pattern

Z-fold pattern is applied to inflatable tube. To validate the simulation method, the one-point fold tube in reference[13] is analyzed and compared to the analysis result provided in the reference. Each part of depolyment exiperiment model for this one-point tube is shown in Fig 9,10.

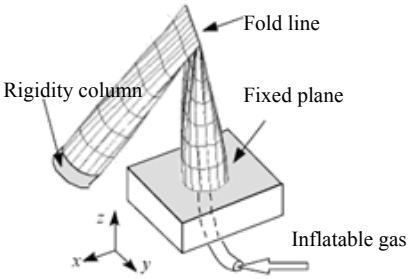

Fig 9: experiment component

Fig 10: fold model of analysis

The section redius of the tube is 12mm, the length is 200mm, the thickness is 104 μm, elastic modulus is $1.08\times10^8 N/m^2$, Possion's ratio is 0.3 and the density is $910 Kg/m^3$. The inflatable gas is nitrogen, the temperature of experiment circumstance is 300.68K and the gas constant is $296.798 J/KgK$. The mass of rigidity column shell is 75.7g, The section redius is 15m and the thickness is 3mm.

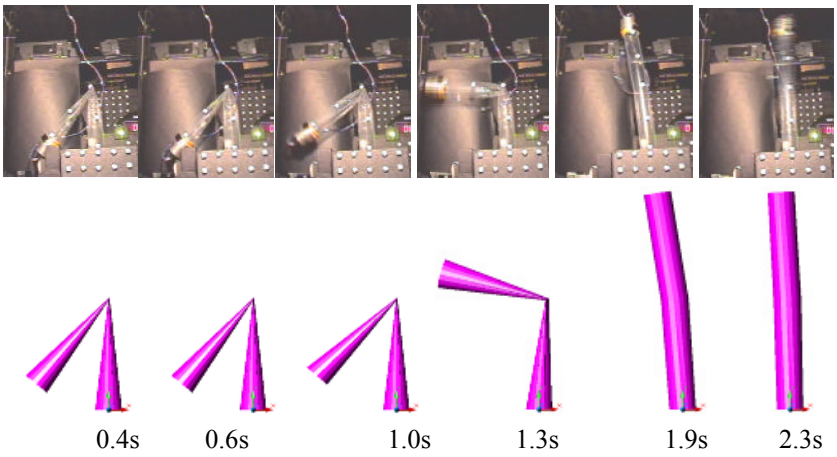

Fig 11: comparion between experiment and analyze result

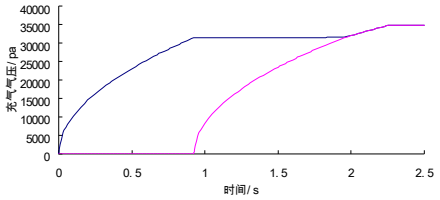

Fig 12: inflatable pressure changes

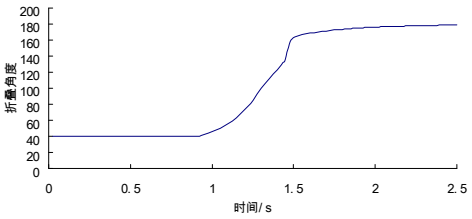

Fig 13: fold angle changes

The pressure of two air chambers changes by depolyment time is shown in Fig 12. At first the pressure of the first air chamber is increasing and the section beween two chambers is opened at time 0.9s. Then the gas come into the second chamber and the pressure is higher. Finally the pressure of two chambers reached to designed pressure 35 kPa. The fold angle between two chamber changes by depolyment time is shown in Fig 13. The initial angle value is 40 degree and become large after 0.9s. Finally the tube become straight and the fold angle become 180 degree.

6.2 curve fold pattern

Inflatable tube is folded by curve fold pattern and the fold configuration is shown in Fig. The gas come into the tube from inferior end and this end is fixed. The tube is divided to 8 chambers and the pressure of each chamber is obtained at each time. Each state during depolyment is shown in Fig 14. The self-collide of membrame film always occurs.

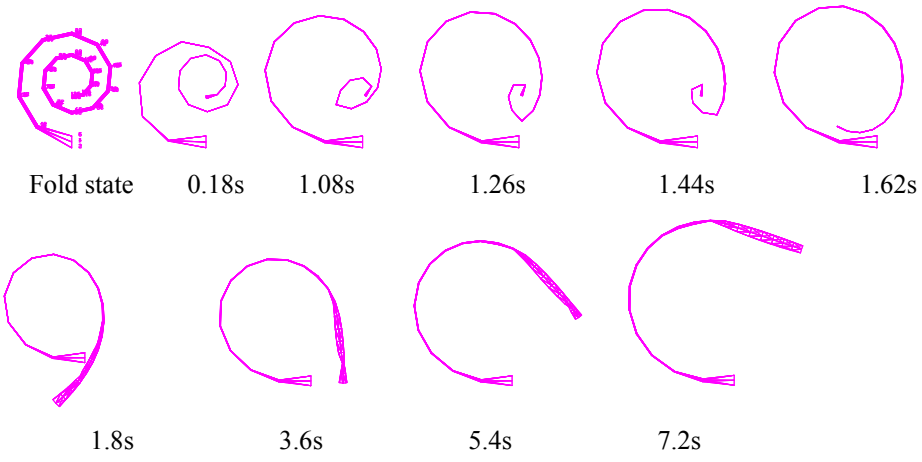

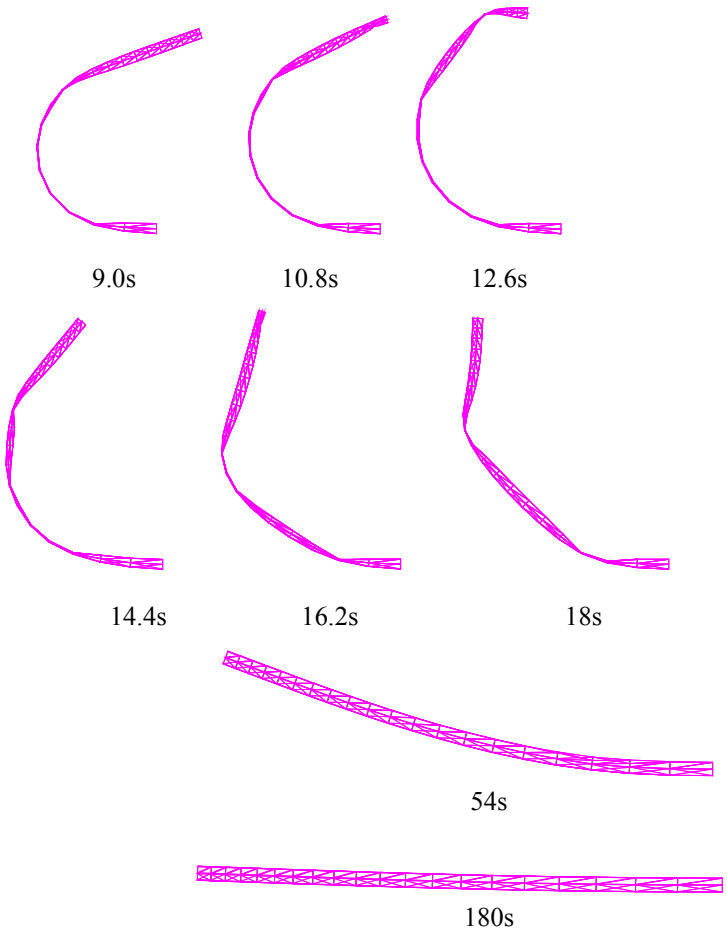

Fig 14: depoly states of inflatable tube

6.3 Whole antenna model

The whole model of inflatable antenna include tube, torus and reflector, just as Inflatable Antenna Experiment(1996, NASA).

The caliber D of reflector is 6m and focus length f is 7.5m. The fold ratio of longitude is 0.5. The different between reflector and canpoy is not consider. The radius of torus axes is 1.8m. The length of single tube is 8.0498m and the section radius is 0.06m. 4 parts is folded by Z-fold pattern. The whole antenna is stowaged into a cylinder volume which radius is 2m and heigh is 2.6m.

There are 24 cables between the reflector and the torus. The membrane material of torus and reflector is Kapton. The elatic modulus is 3.5Gpa, Possion's ratio is 0.35, the

thickness is 0.127mm and the density is 1450Kg/m^3. The material of cable is the Kelver, which diameter is 1.2mm. The elastic modulus of Kelver is 1.31×10^{11}Pa . The element number of torus is 288 and node number is 144. The element number of reflector is 720 and node number is 362. the element number of each tube is 48 and node number is 30. so element number of whole model is 1152 and node number is 596.

The design pressure of torus and tube is 23.6 KPa and the design pressure of reflector is 1Kpa. The pressur isn't change during the deployable process. The non-stress state and flod state of the whole antenna structure is shown in Fig 15,16.

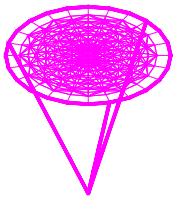

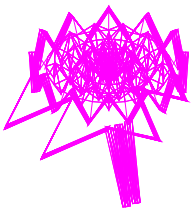

Fig 15: non-stress state of antenna Fig 16: fold state of antenna

The result of simulation

The intersectant point of three tubes is fixed in the satellite. So this point is fixed during simulation. Each deployable state are shown in Fig. At first, the tube and torus is inflatabled. The tube is tend to straight and drive the torus and reflector move along the Z positive coordinate. The reflector is drive to move by cables. The axes of trous is tend to triangle shape drived by tubes in initially and deploy to circle slowly.

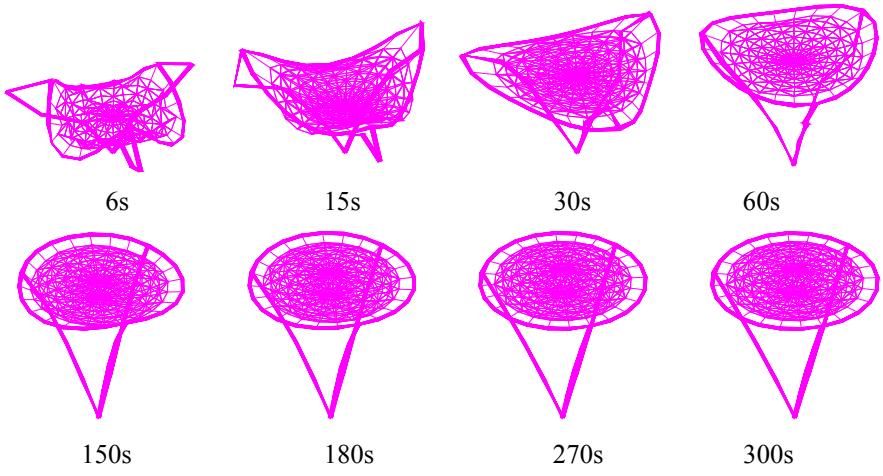

Fig 17: each deployable state

From the result of simulation, three tubes and the axes of torus is deployed fully at 60s. At this time, there are some wrinkle along the section direction of tube. The reflector is

pulled by cables, but there are many wrinkles in the surface. The reflector and the section of torus continue to deploy after 60s. the section of torus deploy fully and keep the shape at 150s. The reflector is move from initial slaw state to final configure slowly subjected to the design pressure. Now the internal force in reflector surface is transferred to the torus by cables. From the result, deformation of the torus is very small.

The deployable process simulation is estimated base on the result. The whole deployable process take 300s (5 min). The shape precision after full deploy is 0.13mm. The large diameter of torus is 7.3252m and small diameter is 7.0855m. The length of tube is 8.0429m. From this, the deploy process of whole antenna is deploying by design pattern and the movement is smooth. The shape precision of full-deployable state is high. This result also validate the simulation method and the fold scheme of inflatable antenna.

7. Conclusion

The simulation method of membrane deployable structure is mentioned based on improved spring-mass system. The distinguish rule of self-contact elements is advanced and penalty function method is used to solve this difficult problem. These time history of inflatable pressure and other gas parameter of each tube part are analyzed. The tube between two hinges is equal to cantilever beams and the moment tending to straighten the tube is obtained. Initial state and fold state of main members of inflatable antenna are described, which include inflatable tube, inflatable torus and reflector etc. Deployable drive forces and deployable process order of each part are analyzed. The antenna model like IAE antenna is analyzed and simulated by the fore mentioned system. Each state during deployment process and velocity and acceleration of each node are obtained. The example is used to validate the simulation method and the fold scheme of inflatable antenna.

References

[1] LIU Ming-zhi and GAO Gui-fang. Advances in the study on structure for space deployable antenna. *Journal of Astronautics*. 2003, 24 (1):82-87.

[2] Cliff E W and Ron C S. A hybrid inflatable dish antenna system for spacecraft // Proceedings of the 42th AIAA/ASME/ASCE/AHS/ASC SDM Conference, AIAA -2001-1258. Seattle, WA: AIAA, 2001: 1-9.

[3] John K H L and David P C. An inflatable microstrip reflect array concept for Ka-band applications // Proceedings of the 41th AIAA/ASME/ASCE/AHS/ASC SDM Conference, AIAA -2000-1831. Atlanta, Georgia: AIAA, 2000: 1-13.

[4] David L. Inflatable deployed membrane waveguide array antenna for space[C]// Proceedings of the 44th AIAA/ASME/ASCE/AHS/ASC SDM Conference, AIAA-2003-1649, Norfolk, Virginia: AIAA, 2003: 1-7.

[5] Merthly P J. Numerical Prediction of Deployment , Initial Fill , and Inflation of Parachute Canopies [C] . AIAA - 84 - 0787 ,1984.

[6] Fang H, Liu M and Hah J. Deployment Study of a Self-Rigidizable Inflatable Boom. 44th AIAA/ASME/ASCE/AHS Structures, Structural Dynamics, and Materials Conference, Norfolk, 2003, AIAA-2003-1975:1-9.

[7] Clem A L, Smith S W. A pressurized deployment model for inflatable space strucutures. AIAA-2000-1808:1-11.

[8] Liu Xiaofeng, Tan huifeng and Du Xingwen. Deployment simulation of inflatable space tube. *Journal of harbin institute of technology*, 2004 , 36(5):684-687. (in Chinese)

[9] Haug E, Protard J B and Gerren A M.The Numerical Simulation Of The Inflation Process Of Space Rigidized Antenna Structure Pro-ceedings of The Internation Conference:Spacecraft Strcutures And Mechanical Testing ESA.1991:862-868.

[10] Salama M, Fang H and Lou M. Resistive Deployment of Inflatable Structures. 42nd AIAA/ASME/ASCE/AHS Structures,Structural Dynamics, and Materials Conference, Seattle, 2001, AIAA-2001-1339:1-9.

[11] Wang J T and Johnson A R. Deployment simulation of ultra-lightweight inflatable structures, AIAA-2002-1261: 1-14.

[12] Wang J T and Johnson A R. Deployment Simulation Methods for Ultra-Lightweight Inflatable Structures. NASA/TM-2003-212410 ARL-TR-2973.

[13] Miyazaki Y and Uchiki M. Deployment dynamics of inflatable tube. AIAA-2002-1254:1-10.